JOURNAL OF APPLIED ELECTROCHEMISTRY **28** (1998) 405–410

Characterization of corroding aluminium alloys with electrochemical noise and electrochemical impedance spectroscopy

P. R. ROBERGE

Department of Chemistry and Chemical Engineering, Royal Military College, Kingston, Ontario, Canada, K7K 5L0

D. R. LENARD

Dockyard Laboratory (Esquimalt), Esquimalt Defence Research Detachment, FMO Victoria, BC, Canada, V0S 1B0

Received 18 January 1996; revised 15 April 1997

Electrochemical impedance spectroscopy (EIS) and spontaneous voltage fluctuation measurements were made on three orthogonal faces of 7039-T64 and 2519 aluminium alloy specimens during 10 day exposure periods into aerated 3% NaCl solutions. The spontaneous voltage fluctuations generated by the specimens were analysed with two techniques designed to reveal the stochastic character of these signals and their fractal dimension to establish practical correlation between noise measurements and the degree of pitting of the corroding aluminium specimens. Attempts were made to correlate the results of these analyses with parameters measurable by microscopic examination of the specimens or calculated from EIS measurements. During this study it was found that the slope of the voltage fluctuations and the depression angle of EIS results were both good indicators of the pit density observable on the corroded aluminium specimens.

Keywords: *aluminium alloys*, *corrosion*, *voltage fluctuations*, *impedance spectroscopy*

1. Introduction

A novel technique for the analysis of electrochemical noise generated during the corrosion of metallic specimens was tested during a study of aluminium alloys exposed during 10 days in aerated 3% NaCl solutions. A previous study of electrochemical noise (EN) generated by aluminium sheet material exposed to the same environment had indicated that the departure from a stochastic behaviour, revealed by the stochastic process detector (SPD) method, could be related to the degree of localized corrosion of metallic surfaces [1]. The study of corroding aluminium specimens was found to be ideally suited for testing new noise analysis techniques since the corrosion of aluminium is often localized and has already been the subject of extensive studies [2–8]. In the present paper, the results obtained with three orthogonal faces of 7039-T64 and 2519-T87 aluminium specimens exposed to a saline solution are compared to electrochemical impedance spectroscopy (EIS) measurements and micrographs of exposed specimens.

Fluctuations of potential or current of a corroding electrode are a well known and easily observable phenomenon and the evaluation of EN as a corrosion tool has increased steadily since Iverson's paper in 1968 [2]. The study of EN has repeatedly been found most appropriate for monitoring the onset of events leading to localized corrosion and understanding the chronology of the initial events typical of this type of corrosion. During localized corrosion electrochemical noise is believed to be generated by a combination of stochastic processes, such as passivation breakdown and repassivation events, and deterministic processes which can be caused by film formation or pit propagation processes.

2. Noise analysis

The most traditional way to analyse electrochemical noise data has been to transform time records in the frequency domain to obtain power spectra. Spectral or power density plots would thus be computed utilizing fast Fourier transforms (FFT) [9] or other algorithms such as the maximum entropy method (MEM) [10]. A few studies have indicated that the roll-off of the voltage noise amplitude from corroding electrodes could be a useful characteristic of corrosion processes [11, 12]. In these studies, a roll-off of $-20\,\mathrm{dB\,decade^{-1}}$ was thus associated with pitting attack while one of $-40\,\mathrm{dB\,decade^{-1}}$ was found more characteristic of general corrosion processes. When converted into a spectral density plot a roll-off of $-20\,\mathrm{dB\,decade^{-1}}$ would correspond to a spectral

exponent of 1 and a roll-off of $-40\,\mathrm{dB\,decade^{-1}}$ to an exponent of 2. For stochastic signals, the spectral exponents (β) of spectral density plots can be related to the fractal dimension (D) of the signals with Equation 1 [13]. But since the noise signals often contain deterministic features that can induce variations in the slope of a spectral density plot (SDP), such an analytical method is not the most reliable way to evaluate the fractal dimension of a signal.

$$D = \frac{5-\beta}{2} \tag{1}$$

Another useful mathematical model was proposed to specifically reveal the fractal characteristics of signals [14]. A detailed description of this technique, also called rescaled range analysis or R/S technique (where R or $R(t,s)$ands for the sequential range of the data points increments for a given lag s and time t, and S or $S(t,s)$ for the square root of the sample sequential variance), can be found in Fan *et al.* [15]. Hurst [16] and later Mandelbrot and Wallis [17] have proposed that the ratio $R(t,s)/S(t,s)$ is itself a random function with a scaling property described by Relation 2 where the scaling behaviour of a signal is characterized by the Hurst exponent (H) that can vary between $0 < H < 1$:

$$\frac{R_{(t,s)}}{S_{(t,s)}} \propto S^H \tag{2}$$

It has additionally been shown that the local fractal dimension of a noise trace is related to H through Equation 3, which makes it possible to characterize the fractal dimension of given time series by simply calculating the slope of a R/S plot [18].

$$D = 2 - H \quad \text{for } 0 < H < 1 \tag{3}$$

In contrast with any other signal analysis technique, the SPD technique, which has been described in details elsewhere [1], attempts to quantify the stochasticity of a noise record. The SPD technique consists in two levels of transformation. First, the noise records are transformed into series of singular events, that is, each point of a time series is examined for its appurtenance to either positive or negative noise peaks. In the second level of transformation, the distribution of peak lengths $f(t)$ is examined and compared to the theoretical exponential decay distribution, represented by Equation 4 where λ_t is the mean value and t is the peak length (time), that would characterize a series of stochastic events [19]. The goodness-of-fit (GF) of real data by the exponential function is then calculated to serve as a measure of stochasticity of the time records:

$$f(t) = \lambda_t \mathrm{e}^{-\lambda t} \tag{4}$$

The slopes of the basic events are also computed by the SPD technique since this parameter is thought to be an important characteristic of the electrochemical systems being studied. The main idea behind applying the SPD technique to the analysis of electrochemical noise is the belief that localized corrosion should induce deterministic features in the overall noise signatures. Also, since the SPD technique is particularly sensitive to any digression from purely stochastic signals, such an analysis could serve as an advanced warning method to detect the onset of a localized corrosion situation. But differences between various noise analysis techniques can probably be best illustrated by examining the results one can obtain with synthetic noise files. For such a comparison the readers are referred to a previous publication in which synthetic noise files were analysed by the SPD and R/S techniques and the results compared to the analysis with FFT [20].

3. Experimental details

Two aluminium alloys designed for armour and structural applications, 7039-T64 and 2519-T87, were used in this study. The specimens, with analysed compositions presented in Table 1, were cut from the plate material (thickness 3 cm) and mounted in epoxy according to metallographic techniques. The average exposed area, for the 28 specimens prepared in this study, was calculated to be $1.14\ (\pm 0.1)\,\mathrm{cm^2}$ (Table 2). The samples were mounted in a manner that would expose only one face of each of three orthogonal planes related to the rolling direction of the plate material (LT, SL and ST). A total of fourteen 10 day exposure experiments were carried out in this study of structural aluminium exposed to 3% NaCl solutions. Three of these experiments were carried out by exposing specimens revealing the three faces of the 7039 alloy while many of the other eight experiments were carried out with the 2519 alloys as replicates to verify the reproducibility of such measurements, that is, three experiments with exposed LT material, six with SL, and two with ST.

Prior to mounting, provisions were made for an electrical connection to the unexposed back of the samples. The unexposed edges were coated with an aluminium-vinyl anti-corrosive paint to prevent crevice corrosion between the epoxy mount and the aluminium electrodes. After mounting, the specimens were polished (using 240, 400 and finally 600 grit papers) and cleaned with acetone and dichloromethane.

Table 1. Analysed compositions (%) of the aluminium alloys tested

	Cr	*Cu*	*Fe*	*Mg*	*Mn*	*Ni*	*Si*	*Ti*	*V*	*Zn*	*Zr*
2519-T87	nd*	5.6	0.15	0.19	0.28	nd*	0.06	0.06	0.05	0.07	0.19
7039-T64	0.53	0.52	0.53	1.96	0.74	0.24	0.13	0.02	0.01	15.8	nd*

* not detected.

Table 2. Average results of the E_{corr} values and calculated from EIS measurements

Alloy	*Face*	*Exp*	*A* /cm^2	R_p /kΩ cm^2	C_{dl} /μF cm^{-2}	*CPE**	*CR*† /μm y^{-1}	E_{corr} /mV vs SCE
7039	LT		1.13	31 (42)‡	5.1 (27)	0.90 (36)	8	−896 (3)
	SL		1.20	24 (47)	5.8 (18)	0.90 (31)	10	−884 (2)
	ST		1.01	13 (32)	7.7 (30)	0.91 (44)	20	−880 (2)
2519	LT	1	0.93	6.0 (19)	150 (68)	0.74 (19)	40	−713 (3)
		2	1.12	4.1 (26)	140 (27)	0.77 (13)	60	−723 (2)
		3	1.09	4.6 (14)	140 (18)	0.76 (7)	60	−724 (2)
	SL	1	1.30	3.9 (25)	220 (30)	0.75 (21)	70	−716 (1)
		2	1.43	3.2 (18)	360 (18)	0.74 (19)	80	−709 (1)
		3	1.46	4.1 (34)	260 (19)	0.78 (31)	60	−725 (3)
		4	1.33	3.4 (23)	180 (16)	0.77 (24)	80	−723 (3)
		5	1.23	3.8 (18)	180 (22)	0.79 (25)	70	−739 (4)
		6	1.57	3.5 (25)	220 (35)	0.79 (41)	70	−725 (4)
	ST	1	1.23	4.4 (24)	160 (23)	0.81 (30)	60	−728 (1)
		2	1.22	4.2 (17)	200 (39)	0.82 (20)	60	−718 (1)

* constant phase element.
† corrosion rate calculated using Equation 7, i.e. same precision as R_p.
‡ relative standard deviation (%).

3.1. *Electrochemical impedance spectroscopy*

For each experiment, a pair of identical aluminium specimens (same exposed face) were immersed in a 2 l beaker containing a solution of 3% sodium chloride at ambient temperature (22 ± 2 °C). Each cell was equipped with an air purge, to keep the solution saturated with air, and a saturated calomel electrode (SCE) brought into close proximity with one electrode by a Luggin probe (Fig. 1). The mounted specimens were separated by 2.5 mm and kept in a stable parallel position with plastic holders. The electrochemical impedance spectroscopy (EIS) measurements were performed with a commercial generator/analyser (Solartron model 1255) at the corrosion potential and in the direction of increasing frequency. A potentiostat was not used in these measurements. The alternating voltage was applied directly between the two aluminium electrodes through a 500 kΩ resistance in a circuit described elsewhere [21]. The probing a.c. current was kept at a value which would not cause more than 10 mV difference (peak-to-peak) across the cell.

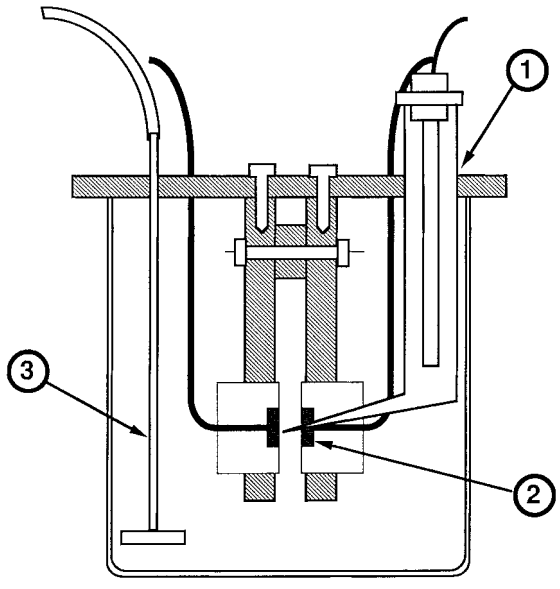

Fig. 1. Schematic description of the electrochemical cell: (1) the reference electrode and its Luggin capillary, (2) exposed metallic specimen and (3) air purge.

3.2. *Electrochemical potential noise*

Standard calomel electrodes (SCE) served to measure the corrosion potential and its fluctuations. The reference electrodes were verified before each experiment and discarded when the values differed by more than 3 mV from another SCE known to be in good condition. The fluctuations themselves were monitored through a high pass filter (10 MΩ resistor in series with a 0.2 mF capacitor, thus having a frequency cut-off (f_c) at 80 μHz, Equation 5), to increase the sensitivity of the measurement technique by blocking off the d.c. voltage. A high precision multimeter, HP model 3457A, was used at its most sensitive scale (i.e., 30 mV with a resolution of 10 nV). A sampling interval (Δt) of 0.5 s was chosen in combination with the high-pass filter to produce the equivalent of a bandpass filter. The frequency domain corresponding to these sampling conditions can be evaluated to be between 1 Hz (f_{max}), Equation 6, and 80 μHz (f_c).

$$f_c = 1/2\pi RC \quad (5)$$

$$f_{max} = 1/2\Delta t \quad (6)$$

Each EN data gathering was completed before starting the EIS measurements to avoid any obvious perturbation. A computer controlled multiplexer sequentially directed the inputs from each technique to a storage device. At the completion of these experiments, the specimens were removed and examined with optical microscopy.

4. Results and discussion

The corrosion rates, double layer capacitance (C_{dl}) and constant phase element (CPE) values were

calculated from the EIS measurements. The transformation of the R_p values into approximate corrosion rates was possible by using Equation 7, after correcting for the two electrode configuration (each electrode $= R_p/2$). In Equation 7, EW is the equivalent weight of the corroding metal ($8.99\,g\,eq^{-1}$ for aluminium alloys), d the metal density ($2.7\,g\,cm^{-3}$), A the exposed surface area (cm^2), K is a constant which has a value of 3.3 if R_p is in kΩ and the polarization resistance constant (B) in mV. A B value of 24 mV has been reported as an average value for aluminium alloys exposed to chloride solutions [22].

$$\text{Corrosion rate } (\mu m\,y^{-1}) = \frac{K \times EW \times B}{d \times R_p \times A} \qquad (7)$$

Although Equation 7 can give a good estimate of corrosion rates when such corrosion is uniform, it has to be used with caution when corrosion proceeds in a localized manner since the electrochemical response of a surface will then be affected in ways that are impossible to quantify. The average results of the E_{corr} values as well as the results obtained by the analysis of EIS measurements are presented in Table 2, and the average results obtained by analysing EN records with both the SPD and R/S techniques in Table 3. A few of these experiments were in fact duplicates. For example, the testing of 2519 SL specimens was repeated six times. This was considered to be an important consideration since the reproducibility and repeatability of the results, particularly those obtained with EN, is essential to estimate the significance and practicality of any correlation.

From the average values presented in Tables 2 and 3 it is obvious that both alloys behave quite differently. Table 4 describes the overall observed behaviour per alloy and per parameter reported. Looking at each alloy separately, one can see that the corrosion rates presented in Table 2 indicate that the 7039 specimens corroded much less at its LT and SL faces than at its ST face while the CPE values was almost invariant for all three cases (~0.9) and the C_{dl} values were low for all samples tested (~6 $\mu F\,cm^{-2}$). The corrosion rates ranked quite differently in the case of the 2519 specimens with the ST specimens corroding ($59\,\mu m\,y^{-1}$) similarly to the LT ($53\,\mu m\,y^{-1}$) specimens and less than the SL specimens ($70\,\mu m\,y^{-1}$). The CPE values calculated in these experiments did not vary very much, with LT ≈ SL < ST. The C_{dl} values differed more markedly (i.e., LT < ST ≪ SL).

The means and relative standard deviations calculated from the average of the six 2519 SL experiments presented in Table 2 (R_p 3.65 ± 0.3 or 9%; C_p = 240 ± 67 or 28%; CPE = 0.77 ± 0.02 or 3%; E_{corr} = 723 ± 10 or 1.4%) indicate that for both R_p and CPE the variability between experiments is smaller than the variability within each experiment and does not vary for the C_{dl} values. A surprising result of this analysis was the higher degree of variability (1.4%) of E_{corr} values between experiments than within each experiment (1–4%). Since great care was taken to use calibrated reference electrodes, this discrepancy would be indicative of differences in the surface chemistry of these apparently identical experiments. One plausible explanation of this phenomenon could be the dissolution of intermetallics containing copper since the presence of dissolved copper is known to affect greatly the E_{corr} of aluminium alloys by forcing it towards the pitting potential [23, 24]. The evidence of the specific dissolution of particulate material was on all 2519 specimens examined by optical microscopy during this study (Fig. 2(a) and (b)).

As evidenced by those micrographs, the 2519 alloy corroded by two different pitting modes: one general pitting mode that seemed to affect most of the exposed surface area of the material and a second mode that appeared to be related to the presence of surface

Table 3. Average of the results of EN analysis and percentage of pitted specimen area

Alloy	*Face*	*Exp*	*100-GF** /%	$1/\lambda$ (0.5 s)	*Slope* (+) /$\mu V\,s^{-1}$	*Slope* (−) /$\mu V\,s^{-1}$	$H^{\dagger}$	*Pitted*‡ /%
7039	LT		2.3 (85)§	1.7 (20)	2020 (90)	2130 (90)	0.42 (20)	3
	SL		1.4 (70)	1.6 (20)	2250 (100)	2300 (100)	0.44 (33)	12
	ST		1.7 (70)	1.5 (50)	755 (130)	750 (150)	0.42 (22)	14
2519	LT	1	4.9 (60)	1.2 (15)	3.5 (20)	3.4 (35)	0.26 (10)	69
		2	5.2 (75)	1.2 (20)	4.0 (25)	4.0 (40)	0.22 (10)	68
		3	8.6 (60)	1.3 (10)	4.0 (20)	4.3 (40)	0.24 (15)	68
	SL	1	9.8 (140)	1.4 (25)	3.8 (30)	4.3 (50)	0.22 (50)	67
		2	4.4 (120)	1.5 (30)	3.6 (40)	4.0 (40)	0.26 (20)	65
		3	11 (100)	1.3 (15)	3.6 (15)	4.0 (30)	0.21 (15)	65
		4	11 (100)	1.4 (20)	3.9 (30)	4.6 (50)	0.23 (30)	65
		5	4.4 (80)	1.5 (40)	3.3 (10)	3.5 (15)	0.30 (20)	65
		6	8.9 (70)	1.8 (15)	6.1 (80)	6.3 (65)	0.26 (9)	65
	ST	1	1.9 (60)	1.0 (6)	2.7 (4)	2.6 (4)	0.23 (10)	57
		2	2.6 (50)	1.1 (8)	3.0 (5)	2.8 (6)	0.22 (9)	61

* goodness-of-fit (GF), mean ($1/\lambda$), positive and negative slopes analysed by SPD.
† Hurst exponent obtained by R/S analysis.
‡ ratio of pitted/total area estimated by optical microscopic examination.
§ relative standard deviation (%).

Table 4. Mean values calculated for all parameters involved in the study of the corrosion of 7039 and 2519 aluminium specimens

Alloy/parameter	*7039*	*2519*
R_p ($k\Omega\,cm^2$)	23	4.1
C_{dl} ($\mu F\,cm^{-2}$)	6.2	200
CPE	0.90	0.77
E_{corr} (mV vs SCE)	−887	−722
100-GF (%)	1.8	6.6
$1/\lambda$ (0.5 s)	1.6	1.3
Slope ($\mu V\,s^{-1}$)	1700	3.9
H	0.43	0.24
Pitted area (%)	9.7	60

inclusions or precipitates. The second pitting mode, which was characterized by very deep pits surrounded by apparently unaffected area. By comparison, the 7039 specimens were much less attacked. Figure 3(a) and (b) illustrate the appearance of one of the most pitted specimens of the experiments with the 7039 alloy (i.e., the ST specimens). It can be seen that, even in such case, the pits occupied only a fraction of the surface with no apparent relation to the presence of surface inclusions or precipitates.

The average of all the results obtained by analysing the EN records gathered during these series of tests are presented in Table 3 along with the fraction of pitted surface area observed by microscopic examination of the specimens after their exposure. The analysis of the results presented in Table 3 combined with a comparison of the daily results obtained with EN and other measurements has permitted to establish some interesting correlations between EN analysis of different kinds and the EIS results. In the case of the 7039 specimens, all EN records exhibited a high degree of stochasticity (goodness of fit, $GF \sim 98\%$) even during the first hours of exposure, something unprecedented in this laboratory [1, 20, 25, 26]. The means of the peak populations estimated by the SPD method ($1/\lambda = 1.6 \times 0.5$ s) correlated quite well, in this particular case, with the Hurst exponent calculated by R/S analysis and the R_p values obtained from EIS results (correlation coefficients = 0.8). The fractal dimension (D) estimated from H with Equation 3 indicates that these EN records would be almost perfectly brownian ($D = 1.57$) and have spectral exponent of 1.9 on a power spectrum density plot, an indication of general corrosion [12].

The ratio of apparently pitted area was rather small (3%) for the LT specimens and higher for the SL and ST specimens (i.e., 12 and 14%, respectively). The electrochemical surface activity, indicated by the slopes obtained with the SPD analysis, followed a different order with SL > LT ≫ ST. But no anisotropy was observed between the positive and negative

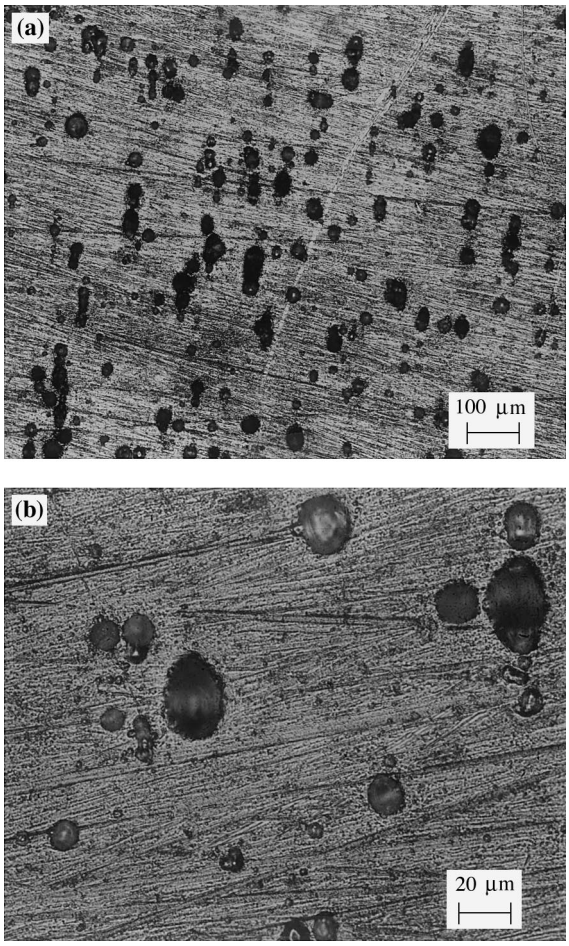

Fig. 3. Optical micrographs of corroded 7039 aluminium specimens: (a) ST, 70×; (b) ST, 350×.

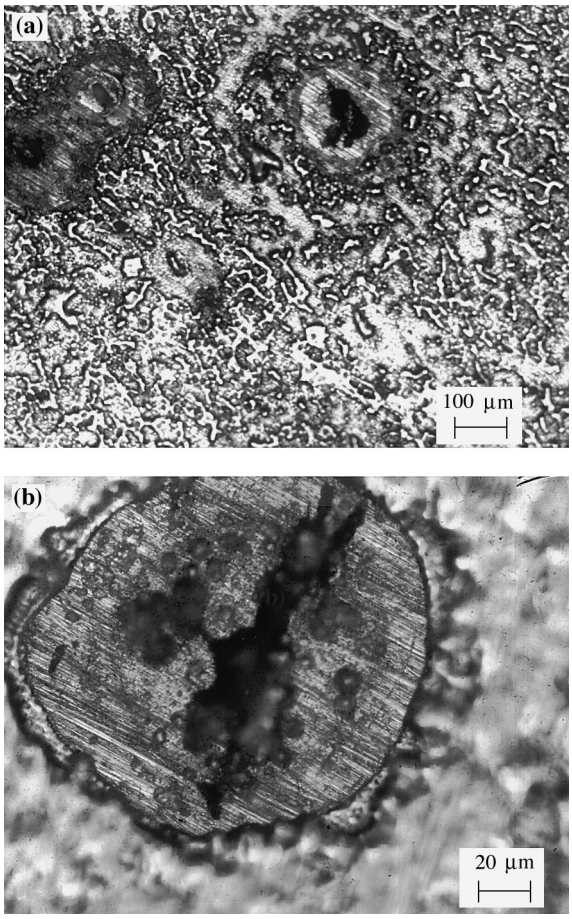

Fig. 2. Optical micrographs of corroded 2519 aluminium specimens: (a) LT, 70×; (b) SL, 350×.

slopes obtained with the 7039 specimens while the negative slopes obtained by SPD of the 2519 EN records were slightly higher than the positive slopes (3.98 vs 3.77 $\mu V s^{-1}$). The large number of experiments used to estimate these averages makes even such a small difference significant and indicative of differences in the anodic and cathodic processes occurring during the corrosion of the 2519 specimens. On the other hand, the values of the slopes calculated for the 2519 EN records were drastically smaller than those obtained with the 7039 specimens, that is, 3.9, 4.3 and 2.9 $\mu V s^{-1}$ for the LT, SL and ST specimens.

The EN records obtained with the LT and SL 2519 specimens were systematically much less stochastic ($GF = 94\%$ for LT and 92% for SL) than the signals gathered with the 7039 specimens or during the experiments with the 2519 ST specimens which also appeared to be well fitted by the SPD model ($GF = 98\%$). The means of the peak populations estimated for the experiments with the 2519 alloy were in average lower than those obtained with the 7039 specimens (i.e., LT $\approx 1.2 \times 0.5$ s, SL $\approx 1.5 \times 0.5$ s, ST $\approx 1.0 \times 0.5$ s), but they did not correlate well with the Hurst exponents calculated with the R/S technique. The Hurst exponents calculated from the EN records gathered with the 2519 alloy (i.e., LT = 0.24, SL = 0.25, ST = 0.23) corresponded to spectral exponents on power spectrum density plots indicative of the presence of pitting corrosion [11, 12].

The pitted area was much more important for all the exposed 2519 specimens than for the 7039 alloy (i.e., 60% vs 10% in Table 4) and, as indicated earlier, the 2519 alloy suffered deep pitting of the surface not experienced by the 7039 alloy.

5. Conclusion

The physical and electrochemical results gathered during the study of corroding 2519 and 7039 structural aluminium indicated that the two materials corrode by very different mechanisms. The large number of data can help to establish the correlations necessary to understand the significance of many of the parameters that can be calculated from EN and EIS measurements. Although the reasons behind the fundamental behaviour of many of the parameters presented in this study are still not fully understood, it appears that some of the key parameters revealed by the analysis of EIS and EN results are directly related to the severity of localized attack of the aluminium material, that is, EN records with low GF and Hurst exponents and EIS measurements with high CPE and C_{dl}.

References

[1] P. R. Roberge, 'The Analysis of Spontaneous Electrochemical Noise by the Stochastic Process Detector Method', *Corrosion* **50** (1994) 502.
[2] W. P. Iverson, *J. Electrochem. Soc.* **115** (1968) 617.
[3] C. Monticelli, G. Brunoro, A. Frignani and G. Trabanelli, *ibid.* **139** (1992) 706.
[4] K. Hladky and J. L. Dawson, *Corros. Sci.* **22** (1982) 231.
[5] U. Bertocci, *J. Electrochem. Soci.* **127** (1980) 1931.
[6] U. Bertocci and J. Kruger, *Surf. Sci.* **101** (1980) 608.
[7] U. Bertocci, *J. Electrochem. Soc.* **128** (1981) 520.
[8] J. C. Uruchurtu and J. L. Dawson, *Corrosion* **43** (1987) 19.
[9] J. S. Bendat and A. G. Piersol, 'Random Data: Analysis and Measurement Procedures', 2nd edn. J. Wiley & Sons, New York (1986).
[10] N. Andersen, 'Modern Spectrum Analysis', IEEE, New York (1978).
[11] K. Hladky and J. L. Dawson, *Corr. Sci.* **21** (1981) 317.
[12] P. C. Searson and J. L. Dawson, *J. Electrochem. Soc.* **135** (1988) 1908.
[13] H. O. Peitzen and D. Saupe, 'The Science of Fractal Images', Springer-Verlag, New York (1988), pp. 71–94.
[14] B. B. Mandelbrot and J. W. van Ness, *SIAM Rev.* **10** (1968) 422.
[15] L. T. Fan, D. Neogi and M. Yashima, 'Elementary Introduction to Spatial and Temporal Fractals', Springer-Verlag, Berlin (1991).
[16] E. H. Hurst, 'Methods of Using Long-term Storage in Reservoirs', *Proc. Inst. Civil Eng.* **5** (Part I) (1956) 519.
[17] B. B. Mandelbrot and J. R. Wallis, *Water Resources Res.* **5** (1969) 321.
[18] J. Feder, 'Fractals', Plenum, New York (1988).
[19] R. E. Walpole and R. E. Myers, 'Probability and Statistics for Engineers and Scientists', 4th edn., Macmillan, New York (1987).
[20] P. R. Roberge, 'Analysis of Spontaneous Electrochemical Noise for Corrosion Studies', *J. Appl. Electrochem.* **23** (1993) 1223.
[21] D. E. Williams and J. Asher, *Corros. Sci.* **24** (1984) 185.
[22] R. Grauer, P. J. Moreland and G. Pini, 'A literature review of polarisation resistance constant (B) values for the measurement of corrosion rate', National Association of Corrosion Engineers, Houston, TX (1982).
[23] S. Furuya and N. Soga, *Corros. Engng* **39** (1990) 79.
[24] H. Bohni and H. H. Uhlig, *J. Electrochem. Soc.* **116** (1969) 906.
[25] P. R. Roberge, D. Lenard, J. G. Moores and E. Halliop, 'Marine Corrosion Behavior of Al-Li Alloy Sheet', *Advancements in Synthesis and Processes*, Society for Advancements of Materials and Process Engineering (1992), pp. M51–62.
[26] P. R. Roberge, E. Halliop, D. R. Lenard and J. G. Moores, *Corros. Sci.* **35** (1–4) (1993) 213.